Lab on a Chip

CRITICAL REVIEW

View Article Online
View Journal

Cite this: DOI: 10.1039/c7lc00037e

Microchip-based single-cell functional proteomics for biomedical applications

Yao Lu,[a] Liu Yang,[b] Wei Wei*[cd] and Qihui Shi*[b]

Cellular heterogeneity has been widely recognized but only recently have single cell tools become available that allow characterizing heterogeneity at the genomic and proteomic levels. We review the technological advances in microchip-based toolkits for single-cell functional proteomics. Each of these tools has distinct advantages and limitations, and a few have advanced toward being applied to address biological or clinical problems that traditional population-based methods fail to address. High-throughput single-cell proteomic assays generate high-dimensional data sets that contain new information and thus require developing new analytical frameworks to extract new biology. In this review article, we highlight a few biological and clinical applications in which microchip-based single-cell proteomic tools provide unique advantages. The examples include resolving functional heterogeneity and dynamics of immune cells, dissecting cell–cell interaction by creating a well-controlled on-chip microenvironment, capturing high-resolution snapshots of immune system functions in patients for better immunotherapy and elucidating phosphoprotein signaling networks in cancer cells for guiding effective molecularly targeted therapies.

Received 11th January 2017,
Accepted 28th February 2017

DOI: 10.1039/c7lc00037e

rsc.li/loc

1. Introduction

Within a biological system, the "genetic codes" are transmitted, processed, integrated and ultimately executed through networks of proteins interacting with one another and with other biologically relevant molecules inside cells. Proteins are key executors of biological processes and connect genomic information to biological functions, including providing cellular structure, transporting molecules, catalyzing biochemical processes and regulating signal transduction.[1] Functional proteomics aim to characterize abundances, post-translational modifications (PTMs) and kinetics of proteins involved in disease progression, immune response, cell differentiation and so on. For example, catalytically active kinases and associated effector proteins comprise the intracellular signaling cascades and are often hyperactivated in cancer cells. Secreted cytokines, chemokines and proteases

[a] Dalian Institute of Chemical Physics, Chinese Academy of Sciences, Dalian, China
[b] Key Laboratory of Systems Biomedicine (Ministry of Education), Shanghai Center for Systems Biomedicine, Shanghai Jiao Tong University, Shanghai, China. E-mail: qihuishi@sjtu.edu.cn
[c] Department of Molecular and Medical Pharmacology, David Geffen School of Medicine, University of California, Los Angeles, CA, USA. E-mail: weiwei@mednet.ucla.edu
[d] Jonsson Comprehensive Cancer Center, David Geffen School of Medicine, University of California, Los Angeles, CA, USA

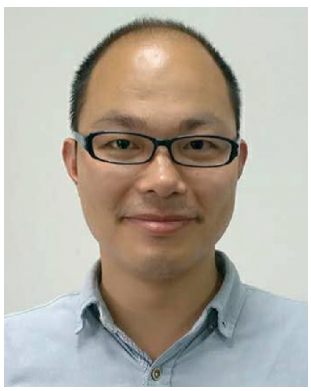

Yao Lu

Yao Lu is an associate professor and group leader of the single cell analysis group at the Dalian Institute of Chemical Physics, Chinese Academy of Sciences. He received his PhD in analytical chemistry from the same institute and completed postdoctoral training at Yale University. His current research is focused on developing microfluidic technologies for single cell analysis and point of care testing with the aim of personalized diagnostics and medicine.

Liu Yang

Liu Yang is a research scientist at the Key Laboratory of Systems Biomedicine and School of Biomedical Engineering in Shanghai Jiao Tong University. She received her B.S. and Ph.D. from Shanghai Jiao Tong University and completed postdoctoral training at the same institution. Her research is focused on developing technologies for automated single-cell identification and manipulation.

are commonly associated with immune cell functions. Traditional methods on protein measurement such as western blotting, mass spectrometry and enzyme linked immunosorbent assay (ELISA) are population-based approaches that may mask the underlying molecular heterogeneity, as even genetically identical cells respond variably to the same cues.[2] Non-genetic cellular heterogeneity has been increasingly recognized as a key feature of many processes of great interest,[3] such as cancer metastasis,[4] tumor cell responses to drugs,[5–7] developmental biology,[8] stem cell differentiation[9] and immune response.[10] For example, varying levels of Sca-1 protein in haematopoietic stem cells were found to determine the timing and type of stem cell differentiation.[9] In a clinical context, T cell populations previously thought to be homogeneous were found to contain subpopulations with different cytokine secretion profiles by single-cell analysis,[10] and these functional differences may serve to predict patient immune response to therapies. Recent technological advances have permitted robust and high-throughput analysis of the genome and transcriptome at the single cell level for characterizing cellular heterogeneity.[1] However, measuring DNA and RNA produces an incomplete picture at the protein level because it fails to provide information on protein PTMs, locations or interactions with other proteins. Importantly, a poor correlation of RNA expression and protein abundance has been reported by a few research groups using single cell analysis.[11–14] For these reasons, single-cell proteomic tools are greatly needed for assaying functional protein activities, including abundances, PTMs, kinetics and interactions with other proteins or biologically relevant molecules.

Single-cell level measurement of protein enables detection of cellular heterogeneity within populations of seemingly similar cells and provides valuable insight into mechanisms that dictate such heterogeneity.[1,15] The functional significance of the observed heterogeneity is determined in two ways. First, the heterogeneous populations can be decomposed into a mixture of simpler, more homogeneous subpopulations that contribute unequally to disease progression or response to therapeutic intervention. In some clinical scenarios, there are behaviors of interest exhibited by only a small subset of cells or even a few outlier cells.[16,17] Population-averaged assays, obviously, fail to resolve these phenotypically distinct subpopulations. Second, the stochastic nature of intracellular events and cell–cell interactions lead to fluctuations of protein levels that are measured across each of many otherwise identical singe cells and not captured by the population-based assays.[18–21] Such fluctuations or heterogeneity in copy numbers of a given protein may contain information regarding the associated protein signaling networks. Determining whether the observed heterogeneity has functional significance requires an analytical framework for quantifying heterogeneity and assessing its information content. Mathematical or statistical physics models with predictive capacity have been developed to interpret the single-cell proteomics data for new biology and strategies for clinical intervention.[22,23]

The biggest challenges to measure functional proteins in single cells are the small amount of protein and the enormous complexity of the proteome. In certain instances, relevant functional proteins such as phosphoproteins are present at low abundance (10^2–10^4 copies per cell).[24,25] In certain clinical scenarios, primary cells (direct from blood or tissue samples) were found to contain significantly lower copy numbers of a given protein than do cultured cells.[23] Single-cell level protein measurement thus requires extremely sensitive assays and minimization of technical error.

Flow cytometry is the most established method for single-cell protein analysis based on fluorophore-labeled antibodies and featured with high levels of throughput and multiplexing.[26] Roederer and Nolan's groups pioneered multi-parameter analysis of 10–15 key proteins associated with signaling pathways in single cells[27–29] and turned cytometry into a powerful tool to semi-quantitatively analyze pathways underlying many diseases[30,31] and for drug screening.[32]

Wei Wei

Wei Wei is an assistant professor at the Department of Molecular and Medical Pharmacology in UCLA David Geffen School of Medicine and a member of UCLA Jonsson Comprehensive Cancer Center. He received his B.S. from Tsinghua University, M.S. from UCSD, and Ph.D. in Materials Science from the California Institute of Technology. He started his appointment as an assistant professor at UCLA after his graduation in 2014. His research interests reside in a highly cross-disciplinary field involving Bio-MEMS, cancer molecular diagnostics/therapeutics and nanomedicine.

Qihui Shi

Qihui Shi is a professor at the Shanghai Center for Systems Biomedicine and School of Biomedical Engineering in Shanghai Jiao Tong University. He received his B.S. from Fudan University and Ph.D. in Chemistry from the University of California, Santa Barbara. Before joining the faculty of Shanghai Jiao Tong University, he worked as a postdoctoral fellow at the California Institute of Technology. His research interests are centered on developing new technologies in single-cell proteomics and single-cell analysis of circulating tumor cells.

Mass cytometry extends the concept of flow cytometry to a substantially higher level of multiplexing through the use of antibodies that are tagged with transition metal mass labels rather than fluorophore labels.[33] A total of 34 parameters, including 31 antibodies, cell viability, DNA content and relative cell size, have been measured in single bone marrow cells at a ~1000 cells per s throughput.[33–35] Image cytometry is another established method for single-cell protein detection based on fluorophore-labeled antibodies and featured with high-throughput due to recent advances in high-content imaging.[36] Because of the spectra overlap of fluorophore-labeled antibodies, image cytometry is limited to the low multiplexing capacity. To overcome this problem, Zrazhevskiy *et al.* reported a multicycle cell staining strategy for measuring more than 20 proteins by multiple staining/de-staining cycles and using semiconductor quantum dots as fluorescent labels.[36] In the same year, Gerdes *et al.* reported a similar fluorophore-inactivated multiplexed immunofluorescence approach to achieve single-cell analysis of 61 protein antigens in 747 human colorectal cancer specimens.[37] Cytometry methods are mainly limited by the cross-reactivity of antibodies and difficulty in assaying secreted proteins.

Different from antibody-based cytometry methods for targeted proteomics, mass spectrometry (MS) is a label-free technology for protein detection and thus has the potential to provide quantitative analysis of the entire proteomics.[38] The label-free feature of MS allows the untargeted (discovery) mode to identify key functional proteins without prior knowledge. Continuous efforts have been devoted to transforming MS into a technology of progressively smaller population of cells,[39–44] or even single cells.[45,46] Compared with well-established cytometry methods, single cell MS is in its infancy. It has, however, witnessed vast development in multiplexing, throughput, sensitivity and sample preparation.[45–47] Virant-Klun *et al.* consistently identified ~450 proteins from single human oocytes that have ~100 ng of protein content per cell, and investigated the differential protein expression at the germinal vesicle stage and the metaphase II stage.[45] Lombard-Banek *et al.* developed a bottom-up high-resolution MS platform and protocol to identify 500–800 nonredundant protein groups in single embryonic cells from a 16-cell frog embryo.[46] Besides sensitivity, delivering the proteome of a single cell to a mass spectrometer with minimal protein loss is a major technological challenge for single-cell MS. Highly efficient microchip-based sample preparation platforms and novel coupling mechanisms of microchips to MS have been developed to address this challenge.[48–50] Compared with MS based on a population of cells, single-cell MS is mainly limited by low-abundance protein assays and discovery proteomics.

This article reviews the technological advances in microchip-based toolkits for single-cell functional proteomics. Microchip-based devices have been increasingly utilized as a means to integrate many functions into a single system, handle a small amount of samples with decreased consumption of expensive reagents, subject cells to controlled cues, and precisely manipulate single cells.[51] Microchips enable creation of well-controlled microenvironments for cell incubation and other functional assays including cell migration, motility and deformability that can be correlated with proteomic signatures for each cell assayed. These features of microchips offer unique advantages compared with cytometry methods and single cell MS. Microchip-based toolkits for single-cell proteomics have been rapidly extended and evolved in the past decade. Each of these tools has distinct advantages and limitations, and a few have advanced toward being applied to address biological or clinical problems. Although some reviews on single-cell proteomics have been published,[1,15,22,23,35,52] this review is more focused on recent progress in microchip-based technologies and the new biology learned from single-cell proteomics data sets.

2. Microchip-based single-cell proteomic technologies

The characteristics of a single-cell proteomic assay include multiplexing capacity, throughput, sensitivity and dynamic range. Multiplexing capacity determines the number of proteins assayed in a single cell measurement and throughput determines the number of cells analyzed in parallel. Many platforms measure the abundance of a given protein in relative units, and in some platforms, calibration curves are established to translate analytical signals into protein concentration, or even copy numbers which are required by some information theoretical approaches for gleaning useful biological insights.[53,54] Different single-cell proteomic technologies are reviewed in this section with a discussion of advantages and limitations. The choice of a tool should be based on the biological questions or clinical measurement of interest, and requirements of the sample.

2.1 Microchip-based image cytometry

Image cytometry that relies on cell staining typically assays 3–4 membrane or intracellular proteins per cell because of the spectral overlap of fluorophore-labeled antibodies. Sun *et al.* presented a microfluidic image cytometry platform allowing concurrent measurement of four signaling proteins associated with the PI3K pathway from individual cells taken from brain tumor biopies.[55] To increase the multiplexing capacity, photocleavable DNA labels have been utilized to label antibodies, leading to system-wide profiling on single cells. The Weissleder group tagged antibodies of interest with short (~70-mer) DNA barcodes using a stable photocleavable linker, and thus each antibody has a unique sequence label (Fig. 1A). After barcoded antibody binding to the cells, the photocleavable linkers release the unique DNA barcodes that can then be detected by gel electrophoresis in a semi-quantitative way[56] or hybridizing to fluorescent complementary barcodes for quantification.[57] The quantified barcodes are translated to protein expression levels by normalizing to DNA per antibody and housekeeping proteins. 90 proteins

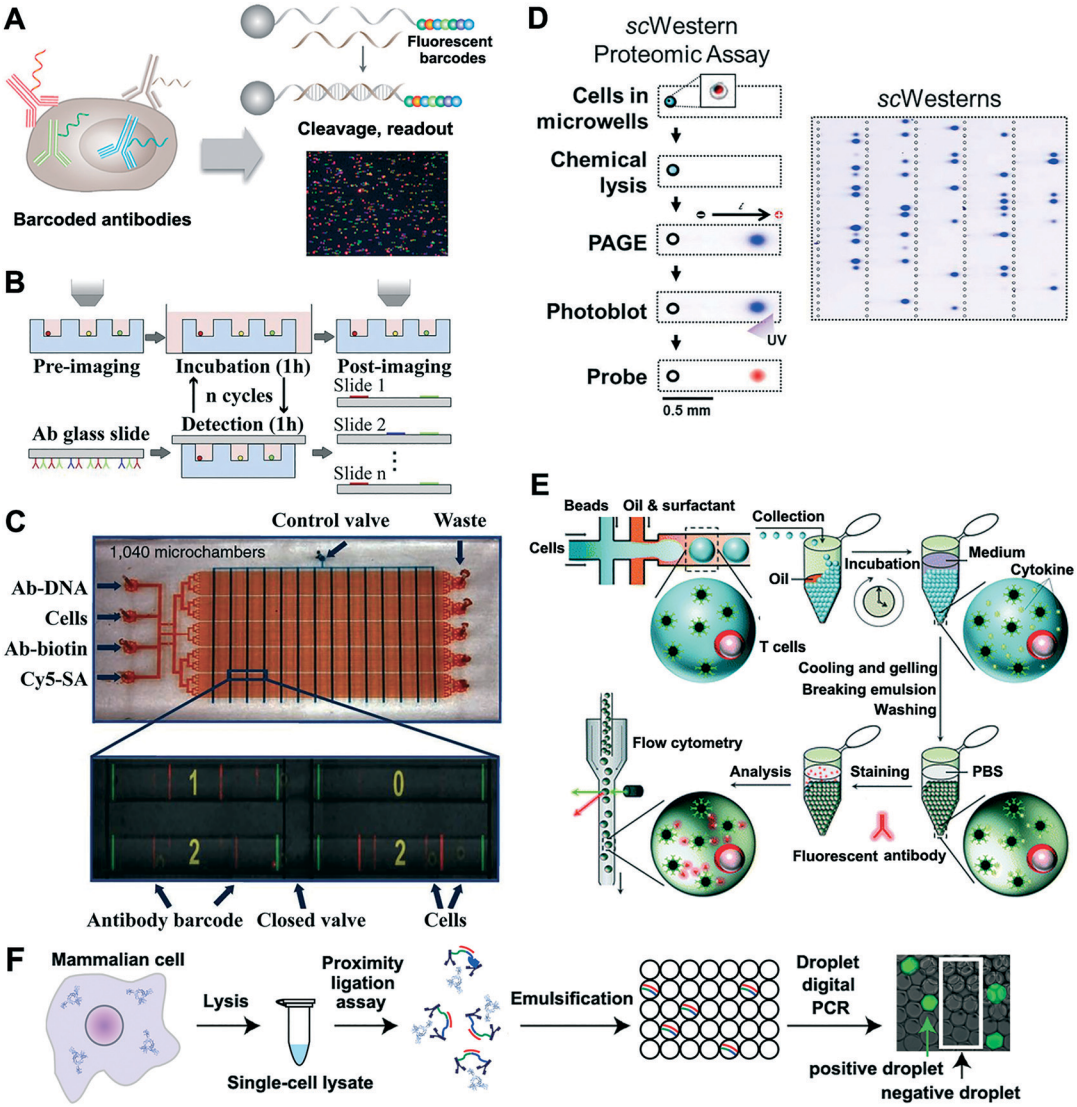

Fig. 1 (A) Schematic representation of the antibody barcoding with photocleavable DNA platform. Protein targets in single cells are labeled with a cocktail of DNA-conjugated antibodies containing a photocleavable linker to allow release of DNA barcodes that can be quantitated by hybridizing to fluorescent complementary barcodes. Reproduced from ref. 57 with permission from the American Association for the Advancement of Science. (B) Assay process flow of the microengraving experiment designed to measure secreted proteins at the single-cell level over time. Single cells isolated in thousands of microwells are incubated with a glass substrate that is microengraved with various antibodies for capture of secreted proteins. The substrate is replaced at various time points to reveal secretion kinetics. Reproduced from ref. 63 with permission from the Proceedings of the National Academy of Sciences. (C) Photograph and fluorescence barcode readouts of the single-cell barcode chip designed for assaying secreted proteins from single cells. The chip is composed of a two-layer microfluidic network that generates thousands of microchambers. Single or a few cells isolated in the microchambers secrete proteins that are captured by antibody barcodes coated on a glass substrate. Four developed barcodes are shown; the yellow number indicates the number of cells in the associated microchamber. Reproduced from ref. 10 with permission from Nature Publishing Group. (D) Single-cell western blotting workflow. The scWestern array is composed of a thin layer of photoactive polyacrylamide gel that houses single-cells in microwells, enables lysis *in situ*, gel electrophoresis, photo-initiated blotting to immobilize proteins and antibody probing for proteomic analyses. Reproduced from ref. 79 with permission from Nature Publishing Group. (E) Work flow of the droplet-based microfluidics for single-cell encapsulation and detection of secreted cytokines. Single T cells are encapsulated in agarose-gel droplets together with functionalized capture beads that capture cytokines secreted from encapsulated cells. The droplets are then gelled and washed to break the emulsion, incubated with fluorescently labeled detection antibodies, and quantified by flow cytometry. Reproduced from ref. 90 with permission from the Royal Society of Chemistry. (F) Proximity ligation assay workflow. In single-cell lysate, two proximity probes bind the target proteins and the connector oligonucleotide hybridizes with the probes followed by formation of a double-stranded DNA. After digestion of proteins by proteases, the remaining dsDNA is detected by droplet digital PCR. Reproduced from ref. 14 with permission from Elsevier.

were profiled at the single-cell level for demonstration of biological variation.[57] This antibody barcoding with photocleavable DNA (ABCD) platform allows co-detection of genetic alternations and protein expression. The ABCD platform reaches the highest level of multiplexing of single-cell proteomic assay, but is limited by the low throughput of parallel

single-cell measurements and the antibody cross-reactivity due to single antibody immunoassay.

2.2 Microengraving method

The Love group firstly used small volume microwells (0.1–1 nL) in an array format to isolate individual cells and quantify secreted proteins by a microengraved (antibody coated) substrate and sandwich-type immunoassay (Fig. 1B).[58–68] Importantly, the microengraved substrate can be replaced multiple times *in situ*, thus enabling kinetic studies of cell secretion at the single-cell level.[62] The technical challenge is the single-cell resolution when a given cell only produces a few thousand or lower copies of a protein of interest. The solution is to enclose cells within a microenvironment with a volume lower than 1 nL. The resultant concentration of the secreted protein is thus sufficiently higher than the detection limit of antibody pairs. Meanwhile, such a small volume of the microwells enables a large number of parallel measurements performed on a single chip. Up to three secreted protein are simultaneously detected using colorimetric discrimination and hybridization chain reaction has been utilized to amplify signals resulting from the sandwich immunoassay, leading to a ~200-fold decrease of detection limit relative to direct fluorescence detection.[61] Numerical simulations have been employed to investigate the transport and binding dynamics of proteins secreted from single cells for increasing the sensitivity and robustness of this microengraving-based, single-cell protein assay.[67] This high-throughput single-cell method allows easy fabrication and assay operation, as well as exhibits the capability of studying secretion dynamics, but is limited by its multiplexing capacity.

2.3 Single-cell barcode chip

A related approach is the single-cell barcode chip (SCBC) developed by the Heath group.[10] The SCBC isolates single cells within 1040 3 nL volume microchambers that contain a miniaturized antibody array, patterned as a barcode for capturing and spatially selective detection of a dozen or so secreted proteins from single cells (Fig. 1C).[10] The key feature of the SCBC is the preparation of miniaturized, spatially encoded antibody barcodes for multiple protein measurement, leading to a high level of multiplexing. The miniature antibody barcodes are created by a DNA-encoded antibody library (DEAL) technology,[69,70] including microfluidics-based flow patterning of a ssDNA barcode and its subsequent conversion into an antibody barcode through a cocktail of antibodies labeled with complementary ssDNA' oligomers. This strategy allows preparation of small-sized, highly uniform antibody barcodes across the entire surface of the glass slide. 20 μm wide DNA strips at a 30 μm pitch are significantly smaller than the standard spotting method. Up to 20 barcode stripes can be patterned in a single microchamber.[69,70] By increasing the number of microchambers on the chip, the throughput of single cell assays can be increased to >1000 with a multiplexing capacity higher than 12.[71,72] Since the cells are randomly distributed in thousands of microchambers on the chip, the number of single-cell microchambers varies and highly depends on the cell loading condition including the cell concentration and flow rate. A higher throughput may induce the increase of chip size but does not result in additional complexity of chip design and operation. For increase of proteins assayed at the single-cell level, the barcode size has to be decreased or other identifiers are introduced for encoding more proteins. Wang *et al.* created a DNA spot array by modifying the DNA barcode patterning method.[73] Each DNA spot has a unique molecular identifier for localizing a labeled capture antibody, enabling spatial encoding of up to 9 antibodies in a 0.15 nL volume microchamber. Lu *et al.* combined spatial (15 barcode locations) and spectral (3 fluorescent colors) multiplexing for double encoding antibodies and thereby up to 45 proteins were co-detected in single cells, representing the highest multiplexing capacity recorded to date for the SCBC assay.[74]

Shi *et al.* modified the initial SCBC design to assay intracellular proteins with single-cell resolution.[75] Each microchamber is constructed with a companion reservoir that contains the cell lysis buffer. When the valve between the cell chamber and the reservoir is opened, the individual trapped cells are lysed and their cytoplasmic proteins are released. The volume of the microchamber is sufficiently small (2 nL) so that many proteins released from single cells are present at detectable levels using miniaturized sandwich immunoassay. The SCBC accommodates 120 separate experiments and a dozen of phosphoproteins and membrane proteins associated with PI3K and Ras/MAPK signaling pathways have been investigated in three isogenic cell lines with different mutation status and under different perturbation conditions.[75] Calibration curves are used to convert the fluorescence readouts to the number of molecules detected. Notably, a careful analysis utilizing both experiment and simulation is performed to evaluate the technical error of this assay (~10%) and determine contributions from biological variation *versus* technical error. The number of parallel measurements is expandable to 320 after optimizing the design of microchambers and controlling the valves.[53,54] A significant advance has been reported by Wang *et al.* with a major modification of the SCBC platform. A valve-less architecture with 8700 0.15 nL volume microchambers was created by employing a set of deformable, three-state poly(dimethylsiloxane) (PDMS) posts for controlling cell loading, on-chip cell lysis and protein assay.[73] Importantly, this SCBC architecture allows simultaneous measurement of secreted, membrane and cytoplasmic proteins, as wells as metabolites from the same single cells, which is a unique advantage. After cell loading in the microchambers, the SCBC is incubated for a period of time, during which certain secreted proteins are captured by the antibody barcodes, followed by on-chip cell lysis and assaying cytoplasmic or membrane proteins that are released. Wei *et al.* measured 5 intracellular proteins (p-EGFR, p-ERK, p-mTOR, p-S6 K, HIF-1α) and three secreted proteins (VEGF, IL-6, MMP-1) simultaneously with single-cell

precision at different oxygen concentrations to investigate how hypoxia conditions influence signaling networks and secretion behaviors of cancer cells.[53] Xue *et al.* quantitated 4 metabolites (c-AMP, c-GMP, GSH, glucose uptake) and 7 metabolism-related proteins (PFK, p-ACAC, p-LKB1, PDK, HK2, PKM2, p-PFKFB2) in single cells separated from the GBM39 neurosphere tumor model under drug perturbations.[76] The metabolic heterogeneity and the correlations between signaling proteins and metabolites yield rich information in cellular metabolic signal regulations. Lu *et al.* correlated the 15-plex cytokine signature with cell motility, a cellular behavior of interest, by an SCBC-based measurement.[71] The SCBC platform has witnessed significant improvement in the multiplexing capacity, throughput and sensitivity since its first debut in 2011, but is limited by the complexity in antibody barcode fabrication and assay operation, low throughput for intracellular protein assay and a lack of high-quality antibody pairs.

2.4 Single-cell protein electrophoresis

Capillary electrophoresis (CE) is a separation-based technique and promising for single-cell analysis. The Zare group developed a microfluidic device that integrates manipulation, lysis, capillary electrophoresis of single cells with single-molecular fluorescence counting for quantifying rare proteins (<1000 copies per cell).[77] However, single-cell micro-scale CE is limited by its low level of throughput and multiplexing capacity. To increase throughput, Dickinson *et al.* developed an automated platform with a throughput of 2.1 cells per min to achieve a fast single-cell CE.[78]

Single-cell western blotting (scWestern) integrates protein electrophoresis and antibody probing, enabling multiplexed protein measurement at the single-cell level.[79] Importantly, scWestern overcomes the antibody cross-reactivity because proteins are first separated by molecular mass (*via* electrophoresis) before the antibody probing step, which allows clear discrimination between on-target and off-target signals.[79–82] In scWestern, a photoactive polyacrylamide gel is coated on a microscope slide and aligned with an array of open-microwells for single cell settling, lysis *in situ*, gel electrophoresis, photo-initiated blotting to immobilize proteins and antibody probing (Fig. 1D). The scWestern technique supports ~2000 concurrent single-cell western blotting assays in <4 h and low starting cell numbers (~200) which is helpful for analyzing rare but biologically important cells. Hughes *et al.* reported a multiplexing capacity of 11 proteins, a linear dynamic range of 1.3–2.2 orders and detection thresholds of ~27 000 molecules, and then applied this technique to study variability in differentiation responses of immature neural stem cells to homogeneous *in vitro* stimuli.[79] Importantly, pERK5, the off-target band for pERK1/2, was identified in scWestern *via* protein electrophoresis, and such an off-target signal was found to contribute up to 52% of the overall pERK signal in unstimulated cells.[79] scWestern analysis is intrinsically well suited for identifying and discarding off-target probing signals. Kang *et al.* later systematically optimized in-well cell lysis and subsequent polyacrylamide gel electrophoresis (PAGE) of a single-cell lysate.[81] Duncombe *et al.* reported material advances of scWestern including a spatially modulated pore-size gradient hydrogel and a dual cross-linked polyacrylamide gel formation.[82] These advances enable thousands of microscale pore-gradient electrophoresis gels to be created on a standard glass slide and importantly, resolve a broad molecular mass range of target proteins.[82] Four HER2-related representative signaling proteins including eIF4E (25 kDa), ERK (44 kDa), HER2 (185 kDa) and mTOR (289 kDa) are therefore assayed at the single-cell level in breast cell lines and tumor biopsy. These signaling proteins span a molecular mass range that encompasses ~80% of mammalian proteome. scWestern detects proteins with high specificity, but exhibits a lower linear dynamic range than other single-cell approaches based on fluorescence readout.

Recently, the Herr group developed a single-cell isoelectric focusing (scIEF) method to measure protein isoforms in individual cells.[83] In the scIEF assay, a 3D microfluidic device is designed to integrate all preparatory and analytical steps, including cell isolation, single cell lysis, isoelectric focusing, UV-actuated blotting and in-gel immunoprobing. The scIEF assay exhibits the ability to resolve isoforms of endogenous proteins from single cells and provides a unique advantage to cytometry methods and other microchip-based tools.

2.5 Droplet-based microfluidics

Microfluidic flow cytometry is not simply a miniaturized version of flow cytometry. It permits analysis of a small number of cells and enables integration of sample handling and single cell analysis on a single microfluidic chip.[84–86] A variant of microfluidic flow cytometry is the droplet-based microfluidics that encapsulates single cells and cytokine-capture beads in droplets, enabling the measurement of proteins released from or secreted by single cells (Fig. 1E).[87–93] Typically, a single cell is encapsulated in 1 pL–2 nL water-in-oil droplets together with fluorescent probes and a functionalized bead. The bead captures secreted proteins and fluorescent probes bind to captured proteins resulting in a bright bead in the droplets for analysis and cell sorting. Debs *et al.* utilized this technique to screen and sort single antibody secreting cells at a high throughput rate.[92] The droplet-based microfluidics overcomes one of the major limitations of traditional flow cytometry that has difficulty in detecting secreted proteins. The recent progress in microfluidics allows generation of droplets at kHz frequencies and reliable encapsulation of single cells into pico- or nanoliter droplets, leading to high-throughput analysis of individual cells.[89] The main limitation of this technique is the background fluorescence in the droplet from the unbound fluorescent labels,

which cannot be removed without breaking the droplet. Instead of water-in-oil droplets, Chokkalingam *et al.* encapsulated T cells and functionalized cytokine-capture beads in monodisperse agarose droplets that were polymerized into hydrogel microparticles by cooling them at 4 °C.[90] The porous nanostructure of gelled agarose microparticles allows bidirectional diffusion of molecules while cells and beads are retained inside the particles. Unbound fluorescent molecules are therefore washed off from agarose microparticles to enhance the detection efficiency. Akbari *et al.* encapsulated cells into alginate microparticles for screening anti-TNF-α antibody-secreting cells from a mixture of hybridoma cells producing anti-myc and anti-TNF-α antibodies.[93] This method prevents the crosstalk between neighboring encapsulated cells and improves the sensitivity.

A unique advantage of droplet-based microfluidics is its capability of linking genotype with phenotype. Target proteins secreted from encapsulated cells are detectable in the droplets; meanwhile, these cells of interest can be sorted and lysed in the droplets for amplification and detection of released DNA or RNA. Droplet-based microfluidics has the major advantage of having high throughput but is limited by its low multiplexing capacity.

The Tay group developed a new approach that combines proximity ligation assay (PLA) and droplet digital PCR (ddPCR) for quantification of both proteins and mRNA in single cells.[14] In a digital PLA, two proximity probes bind the target protein released from lysed single cells, and the connector oligonucleotide hybridizes with the probes, followed by formation of a double-stranded DNA (Fig. 1F). After digestion of proteins by proteases, the remaining dsDNA is then detected and quantitated by ddPCR. This approach was employed to count both endogenous (CD147) and exogenously expressed (GFP-p65) proteins from hundreds of single cells.[14] This approach translates protein detection into DNA detection, and is very similar to the strategy adopted by the Weissleder group.[57]

2.6 Single molecular array

Single molecule array (SiMoA) quantitates the absolute number of proteins with low abundance. SiMoA employs a large number of antibody-coated beads to capture a small amount of proteins and thus realizes single molecules captured on the beads for achieving single-molecule resolution. A microwell chip is then utilized to accommodate these beads, followed by sandwich-type immunoassay for protein detection and enzyme amplification for signal readout. The number of proteins is calculated by counting the beads with amplified signals. Previous work using serum and other biofluids has shown that SiMoA can dramatically improve detection limits and exhibit a wide dynamic range compared to traditional ELISA.[94] This method is thereby qualified for single-cell analysis, for example profiling prostate specific antigen (PSA) expression in single prostate cancer cells.[95] SiMoA is an ultrasensitive assay with absolute quantification of target proteins, but is limited by its low multiplexing capacity, low throughput and high cost for single cell measurement.

3. New biology learned from single-cell functional proteomics

In the following section, we discuss biological and clinical challenges that can be addressed by microchip-based single-cell functional proteomics. These investigations have emphasized types of experiments that are not tractable using traditional population-based assays and other single-cell proteomic technologies such as cytometry methods and single-cell MS.[96]

3.1 Functional heterogeneity and dynamics of immune cells

Cellular immunity is functionally heterogeneous due to a variety of potential pathogen targets. The function of immune cells *in vivo* is mostly defined by the range of proteins they produce. These secreted proteins mediate the tasks of inflammation, target killing, self-renewal, recruitment of other types of immune cells, immune system regulation and so on. Cytometry methods have been utilized to profile cell surface markers, intracellular cytokines and other biomolecules in immune cells.[97] To measure secreted proteins, cytometry methods firstly block protein secretion and then fix and permeablize the cells to allow immunostaining. Blocking of protein secretion is a significant perturbation to cells and assaying intracellular cytokines is not an accurate measure of the function. Microchip-based platforms are able to address this problem and have been utilized to study functional heterogeneity in cellular immunity. Huck and coworkers utilized an agarose droplet-based microfluidics to study cytokine (IL-2, IFN-γ, TNF-α) secretion of single activated Jurkat T cells (Fig. 2A).[90] A total of 7415 cell-containing agarose microparticles were characterized to reveal the presence of 8 different cellular subpopulations. ~85% of Jurkat T cells secreted one or more cytokines and ~57% of Jurkat T cells secreted all 3 tested cytokines upon stimulation and in-droplet incubation. Only 15% of stimulated Jurkat T cells did not secrete any of the tested cytokines. In-depth analysis revealed that cells that secreted large amounts of IL-2 (>10 percentile) also secreted significantly higher levels of TNF-α and IFN-γ. Meanwhile, a population of cells that secreted intermediate levels of IL-2 was observed to produce significantly higher levels of TNF-α. The droplet-based microfluidics provides a high-throughput immune cell phenotyping that unravels the functional heterogeneity and maps subsets within immune cell population with specific functions.

The microengraving method developed by the Love group provides an alternative approach to profile secretion at the single-cell level. Love and coworkers investigated the correlation between cytolysis and cytokine secretion of thousands of individual CD8+ T cells from HIV-infected patients. The

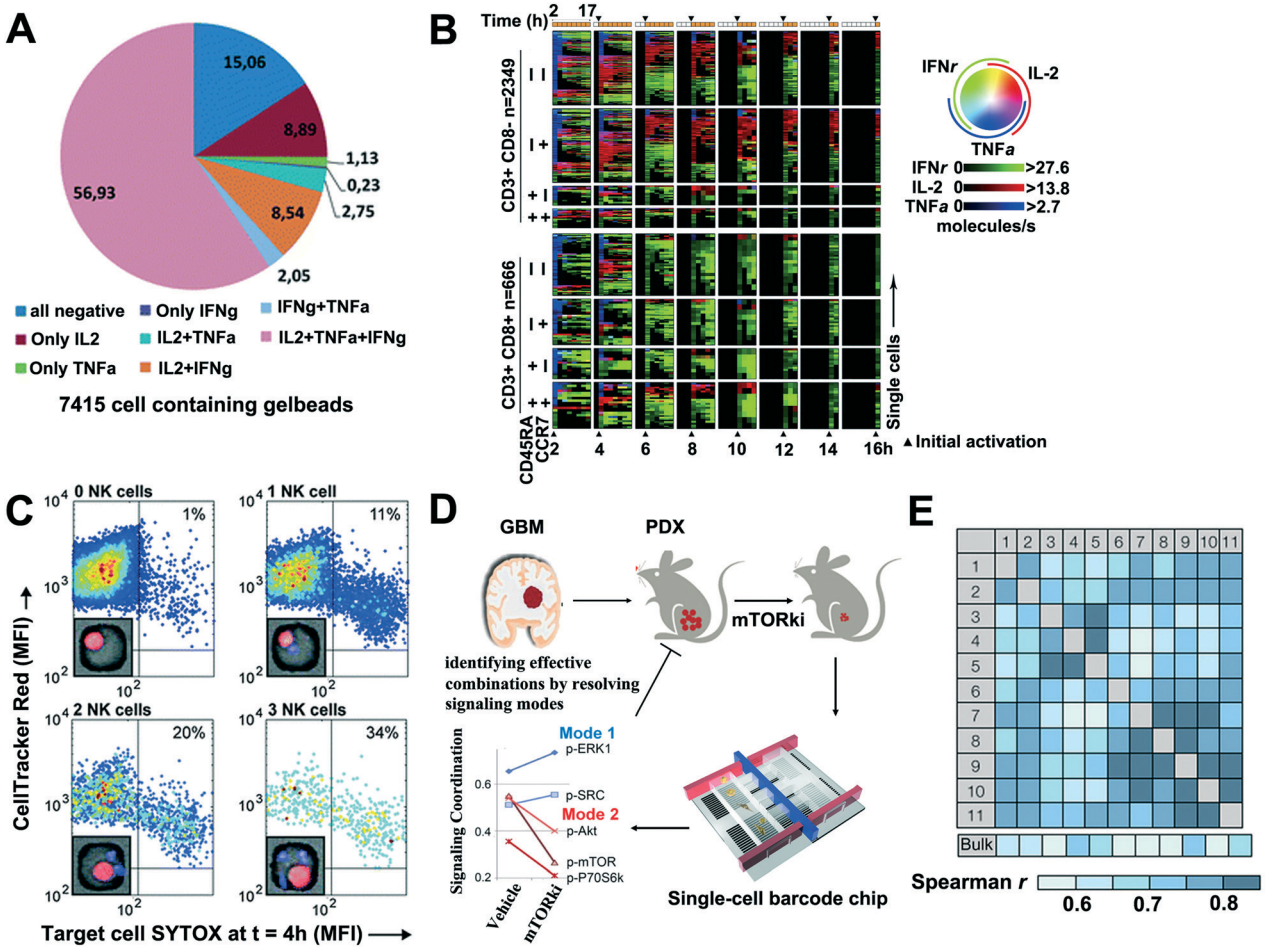

Fig. 2 (A) Jurkat T cells showed heterogeneity in the secretion profiles. 8 sub-populations with different secretion signatures were identified and ~15% of the cells did not secrete any of the tested cytokines. Reproduced from ref. 90 with permission from the Royal Society of Chemistry. (B) Cytokine secretion kinetics of 3015 viable T cells. Each row within each block reflects the dynamic activity of an individual T cell over time. The color wheel illustrates the type and relative magnitude of secreted cytokines; inactivity is black. Reproduced from ref. 63 with permission from the Proceedings of the National Academy of Sciences. (C) NK cells act independently when lysing a single target cell in a nanowell. Representative distribution of SYTOX intensity in target cells after being co-incubated for 4 h in nanowells with one, two, or three NK cells. Data were gated to include wells containing a single target cell. Example images show the initial occupancy of the nanowells for each combination. The percentage of lysed target cells (double-positive for SYTOX and CellTracker Red) is indicated. Reproduced from ref. 67 with permission from the Royal Society of Chemistry. (D) SCBC-based single-cell phosphoproteomics was utilized to analyze patient derived GBM models for identifying shifts in signaling coordination following short-term treatment with kinase inhibitors. This strategy facilitates the design of combinational therapies with reduced drug resistance and enhanced efficacy. Reproduced from ref. 54 with permission from Elsevier. (E) Single-cell proteomic analysis (n = 85 markers, 3 below detection threshold) of 11 single cells in the fine-needle aspirate (FNA) obtained from a lung adenocarcinoma patient. Spearman R correlation coefficient values for each of the single cells relative to each other and to the bulk measurement. Reproduced from ref. 57 with permission from the American Association for the Advancement of Science.

majority of *in vivo* primed, circulating HIV-specific CD8+ T cells were found discordant for cytolysis and cytokine secretion, notably IFN-γ, when encountering cognate antigens present on defined numbers of cells.[62] Importantly the microengraving method permits investigations of kinetics of protein secretion by sequentially replacing, *in situ*, the microengraved slide containing immunoassays. It is a unique feature compared with cytometry methods and other single-cell proteomic methods. For example, Love and coworkers investigated the kinetics of cytokine secretion (IFN-γ, IL-2, and TNF-α) from single primary human T cells by serial microengraving analyses (Fig. 2B).[63] Interestingly, most of the T cells were found to initiate secretion in a monofunctional state, in other words, to release one of the above cytokines at a time rather than maintaining active secretion of multiple cytokines simultaneously. This single cell-based, kinetic assay revealed that T cells follow programmatic, rather than random, patterns of cytokine secretion. This method resolves T cell secretion trajectories and has provided a higher resolution picture of T cell kinetics. In addition, the microengraving method has been utilized to identify rare immune cells with interesting functional properties, such as T cells with efficient antigen-specific responses. These rare cells can be recovered from the sub-nanoliter microwells by

micromanipulation for additional investigations. For example, Love and coworkers assessed HIV-specific T-cell responses and established clonal CD8(+) T-cell lines that represent the most abundant specificities present in circulation using significantly fewer cells than traditional methods.[64]

Tay and coworkers developed a complex microfluidic chip to investigate the kinetics of cytokine secretion and to correlate time-dependent cytokine secretion with transcription factor activity at the single-cell level under dynamic inflammatory inputs.[98] To enable a kinetic assay, antibody-coated beads are firstly moved into chambers to capture secreted proteins released from single cells and then moved out of chambers until the next cycle of bead-based assay. Secreted proteins are quantitated on the chip by conducting bead-based fluorescent sandwich immunoassays with co-detection of the transcription factor from the same single cells. This system was employed to analyze macrophage signal processing under pathogen inputs. The dynamics of TNF secretion were found highly heterogeneous and uncorrelated with the dynamics of NF-kB, the transcription factor controlling TNF production.

Fan and coworkers significantly increased the multiplexing capacity of single-cell secretion assay using a 42-plexed SCBC for studying the cellular functional heterogeneity of differentiated macrophages stimulated with ligands of different Toll-like receptors (TLRs).[74] Several functional subsets (quiescent, polyfunctional fully activated, partially activated) with distinct cytokine profiles were identified by advanced clustering analysis, which demonstrated intrinsic functional heterogeneity in a phenotypically similar cell population. This work shows the potential of SCBC technology for full spectrum profiling of immune functional states in response to the environment or pathogenic stimulations and thereby quantifying functional heterogeneity for accurate immune monitoring.

3.2 Cell–cell interaction

Cells secrete functional proteins in response to not only external stimuli but also their own secreted signals, known as an "autocrine manner", as well as the signals secreted by neighboring cells, known as a "paracrine manner". For this reason, decomposition of the source of signals and studying how cell–cell communication contributes to the functional cell-to-cell heterogeneity are crucial for understanding the immune response. Miller-Jensen and coworkers combined multiplexed, microwell-based single-cell measurements of cytokine profiles with analysis of cytokine secretion by cell populations to determine the role of paracrine signaling in shaping macrophage cells' response to stimulation of Toll-like receptor 4 (TLR4) by lipopolysaccharide (LPS).[99] A system biology model was then established highlighting how cell–cell communication coordinated a rapid innate immune response in the cell population.

The microchip-based method features creating a well-controlled microenvironment for study cell–cell interaction. This is a very unique property of microchips that cannot be accomplished by other single-cell methods. Love and coworkers utilized a microengraved platform to investigate the interactions between natural killer (NK) cells and target cells (*e.g.*, tumor cells, virally infected cells). Secretory responses of NK cells and the resulting cytolytic activity were quantified at the single-cell level (Fig. 2C).[67] They found that NK cells operated independently and promptly when lysing a single target cell and that IFN-γ secretion correlated with low motility for NK cells in contact with a target cell. This study on cell–cell interaction integrates the secretory activity of single NK cells with their cytolytic activity, leading to an improved understanding of the functional heterogeneity of the immune system. Another example was shown by Heath and coworkers who investigated the dynamics of secretion in hundreds of isolated glioblastoma cell pairs and monitored their relative motions over time.[100] The two-cell secretion assays helped to understand how cell–cell communication was coordinating the behavior of cell–cell movement and to identify key proteins most involved in maintaining the free-energy gradient that drove cell–cell motion. Cell–cell signaling was found to depend on the cell–cell separation distance and to influence cellular arrangements in bulk culture. Inhibition of secreted proteins mostly involved in establishing the free-energy gradient was found to cancel the direct motion. Such experiments draw from informative assays combining single-cell proteomics and functional measurements, and may eventually allow complex phenomena within the tissue environment to be understood.

3.3 Immune monitoring of patients undergoing immunotherapy

Cellular immunity is functionally heterogeneous within a cell population defined as relatively homogeneous by surface markers. For capturing and characterizing this functional heterogeneity, single-cell proteomics has been utilized to monitor the functional activity of immune cells taken from patients, for example metastatic melanoma patients participating in an adoptive cell transfer (ACT) trial that uses genetically engineered T cells expressing cancer-specific T-cell receptors (TCRs). In this therapy, the engineered tumor antigen (MART-1)-specific T cells are expanded *ex vivo* and then infused into the patient for driving an anti-tumor immune response. It is therefore crucial to monitor the functional activity and dynamics of the transferred T cells by collecting them at different time points with subsequent profiling of effecter secreted proteins. Ma *et al.* assayed 12 secreted proteins in MART-1-specific CD8+ T cells that were actively responding to tumor and compared them against CD8+ T cells collected from healthy donors.[10] MART-1-specific CD8+ T cells were found to have stronger perforin, IFN-γ and interleukin secretion and a higher level of functional heterogeneity compared with the healthy donor CD8+ T cell controls. Furthermore, Ma *et al.* conducted a kinetic study on three melanoma cancer patients enrolled in the same ACT trial by 19-plexed SCBC

secreted protein assays for monitoring the change of antitumor responses.[101] The adoptively transferred MART-1-specific CD8+ T cells initially exhibit cytotoxicity-dominated antitumor functions that lead to melanoma tissue destruction. Although the tissue destruction results in epitope spreading, the antitumor functions cannot be maintained for a long-term efficacy of TCR-engineering ACT immunotherapy. These studies show that single-cell functional proteomics yields an unprecedented high-resolution view of T-cell functional dynamics in patient-derived samples. The new biology learned from the functional evolution of engineered T cells highlights the need to develop methods for maintaining a long-term antitumor functionality of TCR-engineered T cells.

3.4 Predicting resistance or effectiveness of targeted therapies

Single cell proteomic analysis has been applied to dissect the molecular mechanisms of targeted therapy resistance. In a very recent work,[64] Wei *et al.* identified the rewiring of the signaling network in GBM as a major mechanism of treatment resistance without genome-wide mutation, underscoring the importance of single-cell phosphoproteomics and network rewiring in predicting cancer treatment responses (Fig. 2D).[54,102] The Cancer Genome Atlas (TCGA) on a vast panel of GBM patient samples has identified important genomic alterations in the GBM genome that can be clustered along a set of core druggable pathways with potential drug targets.[103] However, clinical trials with drugs against these alterations or their downstream effectors have yet to favorably impact the outcome for patients, in part because of the emergence of nongenetic, adaptive resistance in tumors. Wei *et al.* used a combined genomic analysis (whole exome sequencing, transcriptome analysis and genomic SNP analysis), stem cell marker tracing and single cell phosphoproteomic analyses to investigate the *in vivo* response of a primary GBM model to an mTOR kinase inhibitor. Neither the genomic analysis nor the stem cell marker tracing supported genetic or phenotypic selection as the dominant resistance mechanism, suggesting an adaptive mechanism of resistance through protein signaling rewiring. The single cell proteomic assays on phosphoproteins associated with major signaling nodes of the hyperactivated pathways of GBM identified by TCGA, coupled to a new computational algorithm, uniquely resolved that while the mTOR kinase inhibitor treatment repressed mTOR signaling and signaling through the PI3k/Akt axis, it also activated signaling through Src and MAPK/ERK. These results further led to the identification of effective (and ineffective) therapies and therapy combinations. Consistent with the prediction, combining the mTOR inhibitor with an ERK inhibitor, a SRC inhibitor, or with both was tested to be effective in preventing tumor growth in mice bearing mTOR inhibitor-resistant GBM, whereas neither any monotherapy nor the combination of ERK and SRC inhibitors was effective. This approach was then generalized to a low-passage EGFR over-expressing patient derived GBM cell line as well as a recurrent GBM patient tumor, fresh from the operation room. A startling new insight of this study is that the adaptive drug resistance may be driven not only by the level of signaling proteins or phosphoproteins downstream of growth factor pathway mutations, but rather by their coordination. In the GBM *in vivo* model of mTOR kinase resistance, the rewiring events were not detected in changes in the phosphoprotein levels until the resistant stage (day 38 following the start of treatment), but were detected by changes in the protein–protein correlation matrix as early as 2.5 days following the start of drug treatment. This suggests that early changes in signaling coordination may be used to anticipate drug resistance, long before full resistance has emerged, thus allowing clinicians to know very quickly on a small biopsy the cellular effectiveness of a treatment strategy.

Weissleder and coworkers utilized the antibody barcoding with photocleavable DNA (ABCD) platform to profile ~90 membrane and intracellular proteins in cancer cells from fine-needle aspirates (FNAs) for mapping inter- and intrapatient heterogeneity in lung cancer at the protein level.[57] Antibody-mediated magnetic selection was firstly employed to isolate EpCAM positive tumor cells from FNAs, followed by micromanipulation to harvest single tumor cells for subsequent proteomic analysis. In one representative patient, the correlation of protein marker expression between 11 single cells and bulk FNAs was varied, ranging from 0.43 to 0.79 (Fig. 2E), that was lower than the correlations between single cells from cell lines and their respective bulk. Even scarce proteins, such as 53BP1 and pH2A.X, were found to be detected at the single cell level. This ABCD platform allows large-scale membrane and intracellular protein profiling of isolated, rare cells for shedding light on cancer heterogeneity which may itself be a biomarker of poor clinical outcome. Furthermore, this platform enables prediction of clinical outcome or identification of promising markers of treatment response by protein profiling on small numbers of cells taken from FNAs. For example, unsupervised clustering of protein profiles from four patients before and after PI3K inhibitor treatment successfully separated out two groups of responders and nonresponders. In five patients with various PI3K mutations and receiving PI3K inhibitor treatment, a marker-ranking algorithm was applied on the measured protein profiles to determine top differential markers for developing better companion diagnostics during the treatment. Dimethylation of histone H3 at Lys79 (H3K79me2) was identified as the top marker, clustered with several other markers including pS6RP (a downstream target of PI3K), pH2A.X (DNA damage marker), PARP (DNA repair protein), and 4EBP1 (protein translation). This cluster best separated responders and nonresponders. Importantly, this cluster covered diverse proteins across various pathways including epigenetic changes, DNA damage, and growth and survival pathways, suggesting the importance of large-scale protein profiling.

4. Conclusions and outlook

The remarkable advances of single-cell functional proteomics provide powerful toolkits for assaying tens of proteins in thousands of individual cells, shedding light on a variety of biological questions that traditional population-based measurement fails to address. These new single cell technologies are now becoming routine in many laboratories, and are improved towards a higher level of multiplexing and throughput, as well as enhancing assay accuracy and robustness for achieving more powerful data sets. From the perspective of exploring the proteome of single cells, the major technical bottleneck is, obviously, the low multiplexing capacity of current single-cell proteomic methods. The cytometry and microchip-based methods exhibit a multiplexing capacity of 10–40 proteins and only the ABCD platform has been reported to assay 90 proteins simultaneously in single cells. However, a panel of tens of proteins represent a very small part of the whole proteome and extensive prior knowledge is thus required in selection of the protein panel before performing single-cell measurements. Upon more proteins assayed and included in the analytical model, the signaling networks are characterized in a more precise way and the predictive capacity of the model becomes more accurate. The low multiplexing capacity of current microchip-based single-cell proteomic methods is attributed to two reasons. First, these methods detect proteins mostly based on highly-specific antibodies that bind their cognate proteins stoichiometrically. The availability of these antibodies is very limited, especially for those methods that require antibody pairs. Antibody cross-reactivity and variability, as well as inadequate cell lines and animal models contribute to non-reproducible findings in preclinical oncology research.[104,105] Second, current antibody-encoding strategies including fluorophores, quantum dots, transition metal mass labels or spatially controlled surface immobilization limit the number of proteins assayed expandable to hundreds or more.

With the increase of multiplexing capacity and assay throughput, single-cell functional proteomics generates high-dimensional single cell data sets that require new analytical strategies and computational tools for gleaning useful biological insights from these data. For example, protein fluctuations and the protein–protein correlations, uniquely resolved by single cell measurements, allow extraction of key information of signaling networks when coupled with appropriate analytical approaches. Single-cell techniques resolve the cellular heterogeneity and clarify the mapping between signaling states and the phenotypes, enabling predictions of the change of signaling states upon environmental and drug perturbations with the help of theoretical advance on understanding single-cell proteomics data.

Microchip-based methods allows making use of very small samples, modulating the microenvironment for cell stimulation, culturing or perturbation, and precisely manipulating single cells, thereby providing a number of compelling advantages in analyzing precious clinical samples. Clinical samples usually contain multiple types of cells and only a small number of cells harbor a feature of interest, leading to key information blurred by bulk-level measurement. Microchip-based methods enable utilization of small samples and identification of rare but biologically important cells from large numbers of background cells. Additionally, microchip-based methods enable integration of sample preparation and proteomic assaying steps in the same platform to reduce sample loss and improve assay automation. These features, obviously, represent unique advantages and great opportunity for biomedical applications of microchip-based proteomics platforms.

Acknowledgements

Q. H. S. is supported by the National Natural Science Foundation of China (Grant No. 81371712) and National Key Research and Development Program of China (Grant No. 2016YFC0900200). W. W. is supported by NIH grant 1U54 CA199090-01 and Phelps Family Foundation. Y. L. is supported by the National Natural Science Foundation of China (Grant No. 21605143), National High Technology Research and Development Program of China (Grant No. 201405003) and funds from the Dalian Institute of Chemical Physics (Grant No. SZ201601).

References

1 J. R. Heath, A. Ribas and P. S. Mischel, *Nat. Rev. Drug Discovery*, 2016, **15**, 204–216.
2 C. Schubert, *Nature*, 2011, **480**, 133–137.
3 S. J. Altschuler and L. F. Wu, *Cell*, 2010, **141**, 559–563.
4 S. Valastyan and R. A. Weinberg, *Cell*, 2011, **147**, 275–292.
5 S. L. Spencer, S. Gaudet, J. G. Albeck, J. M. Burke and P. K. Sorger, *Nature*, 2009, **459**, 428–432.
6 A. A. Cohen, N. Geva-Zatorsky, E. Eden, M. Frenkel-Morgenstern, I. Issaeva, A. Sigal, R. Milo, C. Cohen-Saidon, Y. Liron, Z. Kam, L. Cohen, T. Danon, N. Perzov and U. Alon, *Science*, 2008, **322**, 1511–1516.
7 S. V. Sharma, D. Y. Lee, B. Li, M. P. Quinlan, F. Takahashi, S. Maheswaran, U. McDermott, N. Azizian, L. Zou, M. M. Fischbach and J. Settleman, *Cell*, 2010, **141**, 69–80.
8 J. Wang, H. C. Fan, B. Behr and S. R. Quake, *Cell*, 2012, **150**, 402–412.
9 H. H. Chang, M. Hemberg, M. Barahona, D. E. Ingber and S. Huang, *Nature*, 2008, **453**, 544–547.
10 C. Ma, R. Fan, H. Ahmad, Q. Shi, B. Comin-Anduix, T. Chodon, R. C. Koya, C. C. Liu, G. A. Kwong, C. G. Radu, A. Ribas and J. R. Heath, *Nat. Med.*, 2011, **17**, 738–743.
11 Y. Taniguchi, P. J. Choi, G. Li, H. Chen, M. Babu, J. Hearn, A. Emili and X. S. Xie, *Science*, 2010, **329**, 533–538.
12 S. Darmanis, C. J. Gallant, V. D. Marinescu, M. Niklasson, A. Segerman, G. Flamourakis, S. Fredriksson, E. Assarsson, M. Lundberg, S. Nelander, B. Westermark and U. Landegren, *Cell Rep.*, 2016, **14**, 380–389.

13 A. P. Frei, F. Bava, E. R. Zunder, E. W. Y. Hsieh, S. Chen, G. P. Nolan and P. F. Gherardini, *Nat. Methods*, 2016, **13**, 269–275.
14 C. Albayrak, C. A. Jordi, C. Zechner, J. Lin, C. A. Bischsel, M. Khammash and S. Tay, *Mol. Cell*, 2016, **61**, 914–924.
15 J. R. Heath and M. E. Davis, *Annu. Rev. Med.*, 2005, **59**, 251–265.
16 W. Wang, J. B. Wyckoff, S. Goswami, Y. Wang, M. Sidani, J. E. Segall and J. S. Condeelis, *Cancer Res.*, 2007, **67**, 3505–3511.
17 S. Yegnasubramanian and A. Maitra, *Cancer Discovery*, 2013, **3**, 252–254.
18 A. Raj and A. van Oudenaarden, *Cell*, 2008, **135**, 216–226.
19 P. Paszek, S. Ryan, L. Ashall, K. Sillitoe, C. V. Harber, D. G. Spiller, D. A. Rand and M. R. H. White, *Proc. Natl. Acad. Sci. U. S. A.*, 2010, **107**, 11644–11649.
20 T. L. Yuan, G. Wulf, L. Burga and L. C. Cantley, *Curr. Biol.*, 2011, **21**, 173–183.
21 D. R. Sisan, M. Halter, J. B. Hubbard and A. L. Plant, *Proc. Natl. Acad. Sci. U. S. A.*, 2012, **109**, 19262–19267.
22 W. Wei, Y. S. Shin, C. Ma, J. Wang, M. Elitas, R. Fan and J. R. Heath, *Genome Med.*, 2013, **5**, 75.
23 J. Yu, J. Zhou, A. Sutherland, W. Wei, Y. S. Shin, M. Xue and J. R. Heath, *Annu. Rev. Anal. Chem.*, 2014, **7**, 17.1–17.21.
24 F. Delom and E. Chevet, *Proteome Sci.*, 2006, **4**, 15.
25 M. K. Passarelli and A. G. Ewing, *Curr. Opin. Chem. Biol.*, 2013, **17**, 854–859.
26 L. A. Herzenberg, D. Parks, B. Sahaf, O. Perez, M. Roederer and L. A. Herzenberg, *Clin. Chem.*, 2002, **48**, 1819–1827.
27 S. C. De Rosa, L. A. Herzenberg, L. A. Herzenberg and M. Roederer, *Nat. Med.*, 2001, **7**, 245–248.
28 S. P. Perfetto, P. K. Chattopadhyay and M. Roederer, *Nat. Rev. Immunol.*, 2004, **4**, 648–655.
29 O. D. Perez and G. P. Nolan, *Nat. Biotechnol.*, 2002, **20**, 155–162.
30 K. Sachs, O. Perez, D. Pe'er, D. A. Lauffenburger and G. P. Nolan, *Science*, 2005, **308**, 523–529.
31 J. M. Irish, R. Hovland, P. O. Krutzik, O. D. Perez, Ø. Bruserud, B. T. Gjertsen and G. P. Nolan, *Cell*, 2004, **118**, 217–228.
32 P. O. Krutzik, J. M. Crane, M. R. Clutter and G. P. Nolan, *Nat. Chem. Biol.*, 2008, **4**, 132–142.
33 S. C. Bendall, E. F. Simonds, P. Qiu, A. D. Amir el, P. O. Krutzik, R. Finck, R. V. Bruggner, R. Melamed, A. Trejo, O. I. Ornatsky, R. S. Balderas, S. K. Plevritis, K. Sachs, D. Pe'er, S. D. Tanner and G. P. Nolan, *Science*, 2011, **332**, 687–696.
34 E. Lujan, E. R. Zunder, Y. H. Ng, I. N. Goronzy, G. P. Nolan and M. Wernig, *Nature*, 2015, **521**, 352–356.
35 M. H. Spitzer and G. P. Nolan, *Cell*, 2016, **165**, 780–791.
36 P. Zrazhevskiy and X. H. Gao, *Nat. Commun.*, 2013, **4**, 1619.
37 M. J. Gerdes, C. J. Sevinsky, A. Sood, S. Adak, M. O. Bello, A. Bordwell, A. Can, A. Corwin, S. Dinn, R. J. Filkins, D. Hollman, V. Kamath, S. Kaanumalle, K. Kenny, M. Larsen, M. Lazare, Q. Li, C. Lowes, C. C. McCulloch, E. McDonough, M. C. Montalto, Z. Y. Pang, J. Rittscher, A. Santamaria-Pang, B. D. Sarachan, M. L. Seel, A. Seppo, K. Shaikh, Y. X. Sui, J. Y. Zhang and F. Ginty, *Proc. Natl. Acad. Sci. U. S. A.*, 2013, **110**, 11982–11987.
38 J. Cox and M. Mann, *Annu. Rev. Biochem.*, 2011, **80**, 273–299.
39 L. F. Wannders, K. Chwalek, M. Monetti, C. Kunmar, E. Lammert and M. Mann, *Proc. Natl. Acad. Sci. U. S. A.*, 2009, **106**, 18902–18907.
40 L. L. Sun, G. J. Zhu, Z. B. Zhang, S. Mou and N. J. Dovichi, *J. Proteome Res.*, 2015, **14**, 2313–2321.
41 E. T. Jansson, T. J. Comi, S. S. Rubakhin and J. V. Sweedler, *ACS Chem. Biol.*, 2016, **11**, 2588–2595.
42 R. M. Onjiko, S. A. Moody and P. Nemes, *Proc. Natl. Acad. Sci. U. S. A.*, 2015, **112**, 6545–6550.
43 L. Sun, K. M. Dubiak, E. H. Peuchen, Z. Zhang, G. Zhu, P. W. Huber and N. J. Dovichi, *Anal. Chem.*, 2016, **88**, 6653–6657.
44 S. Wang, Z. Kou, Z. Jing, Y. Zhang, X. Guo, M. Dong, I. Wilmut and S. Gao, *Proc. Natl. Acad. Sci. U. S. A.*, 2010, **107**, 17639–17644.
45 I. Virant-Klun, S. Leicht, C. Hughes and J. Krijgsveld, *Mol. Cell. Proteomics*, 2016, **15**, 2616–2627.
46 C. Lombard-Banek, S. A. Moody and P. Nemes, *Angew. Chem., Int. Ed.*, 2016, **55**, 2454–2458.
47 T. J. Comi, T. D. Do, S. S. Rubakhin and J. V. Sweedler, *J. Am. Chem. Soc.*, DOI: 10.1021/jacs.6b12822, article ASAP.
48 J. S. Mellors, K. Jorabchi, L. M. Smith and J. M. Ramsey, *Anal. Chem.*, 2010, **82**, 967–973.
49 M. Yang, R. Nelson and A. Ros, *Anal. Chem.*, 2016, **88**, 6672–6679.
50 X. Wang, L. Yi, N. Mukhitov, A. D. Schrell, R. Dhumpa and M. G. Roper, *J. Chromatogr. A*, 2015, **1382**, 98–116.
51 T. Thorsen, S. J. Maerkl and S. R. Quake, *Science*, 2002, **298**, 580–584.
52 J. Wang and F. Yang, *Expert Rev. Proteomics*, 2016, **13**, 805–815.
53 W. Wei, Q. Shi, F. Remacle, L. Qin, D. B. Shackelford, Y. S. Shin, P. S. Mischel, R. D. Levine and J. R. Heath, *Proc. Natl. Acad. Sci. U. S. A.*, 2013, **110**, E1352–E1360.
54 W. Wei, Y. S. Shin, M. Xue, T. Matsutani, K. Masui, H. J. Yang, S. Ikegami, Y. C. Gu, K. Herrmann, D. Johnson, X. M. Ding, K. Hwang, J. Kim, J. Zhou, Y. P. Su, X. M. Li, B. Bonetti, R. Chopra, C. D. James, W. K. Cavenee, T. F. Cloughesy, P. S. Mischel, J. R. Heath and B. Gini, *Cancer Cell*, 2016, **29**, 563–573.
55 J. Sun, M. D. Masterman-Smith, N. A. Graham, J. Jiao, J. Mottahedeh, D. R. Laks, M. Ohashi, J. DeJesus, K. Kamei, K. B. Lee, H. Wang, Z. T. Yu, Y. T. Lu, S. Hou, K. Li, M. Liu, N. Zhan, S. Wang, B. Angenieux, E. Panosyan, E. R. Samuels, J. Park, D. Williams, V. Konkankit, D. Nathanson, R. M. van Dam, M. E. Phelps, H. Wu, L. M. Liau, P. S. Mischel, J. A. Lazareff, H. I. Kornblum, W. H. Yong, T. G. Graeber and H. R. Tseng, *Cancer Res.*, 2010, **70**, 6128–6138.
56 S. S. Agasti, M. Liong, V. M. Peterson, H. Lee and R. Weissleder, *J. Am. Chem. Soc.*, 2012, **134**, 18499–18502.

57 A. V. Ullal, V. Petersin, S. S. Agasti, S. Tuang, D. Juric, C. M. Castro and R. Weissleder, *Sci. Transl. Med.*, 2014, **6**, 219ra9e.
58 J. C. Love, J. L. Ronan, G. M. Grotenbreg, A. G. Van der Veen and H. L. Ploegh, *Nat. Biotechnol.*, 2006, **24**, 703–707.
59 E. M. Bradshaw, S. C. Kent, V. Tripuraneni, T. Orban, H. L. Ploegh, D. A. Hafler and J. C. Love, *Clin. Immunol.*, 2008, **129**, 10–18.
60 Q. Han, E. M. Bradshaw, B. Nilsson, D. A. Hafler and J. C. Love, *Lab Chip*, 2010, **10**, 1391–1400.
61 J. Choi, K. R. Love, Y. Gong, T. M. Gierahn and J. C. Love, *Anal. Chem.*, 2011, **83**, 6890–6895.
62 N. Varadarajan, B. Julg, Y. J. Yamanaka, H. Chen, A. O. Ogunniyi, E. McAndrew, L. C. Porter, A. Piechocka-Trocha, B. J. Hill, D. C. Douek, F. Pereyra, B. D. Walker and J. C. Love, *J. Clin. Invest.*, 2011, **121**, 4322–4331.
63 Q. Han, N. Bagheri, E. M. Bradshaw, D. A. Hafler, D. A. Lauffenburger and J. C. Love, *Proc. Natl. Acad. Sci. U. S. A.*, 2012, **109**, 1607–1612.
64 N. Varadarajan, D. S. Kwon, K. M. Law, A. O. Ogunniyi, M. N. Anahtar, J. M. Richter, B. D. Walker and J. C. Love, *Proc. Natl. Acad. Sci. U. S. A.*, 2012, **109**, 3885–3890.
65 Y. J. Yamanaka, G. L. Szeto, T. M. Gierahn, T. L. Forcier, K. F. Benedict, M. S. Brefo, D. A. Lauffenburger, D. J. Irvine and J. C. Love, *Anal. Chem.*, 2012, **84**, 10531–10536.
66 A. J. Torres, A. S. Hill and J. C. Love, *Anal. Chem.*, 2014, **86**, 11562–11569.
67 Y. J. Yamanaka, C. T. Berger, M. Sips, P. C. Cheney, G. Alter and J. C. Love, *Integr. Biol.*, 2012, **4**, 1175–1184.
68 A. J. Torres, R. L. Contento, S. Gordo, K. W. Wucherpfennig and J. C. Love, *Lab Chip*, 2013, **13**, 90–99.
69 R. Fan, O. Vermesh, A. Srivastava, B. K. H. Yen, L. Qin, H. Ahmad, G. A. Kwong, C. C. Liu, J. Gould, L. Hood and J. R. Heath, *Nat. Biotechnol.*, 2008, **26**, 1373–1378.
70 Y. S. Shin, H. Ahmad, Q. Shi, H. Kim, T. A. Pascal, R. Fan, W. A. Goddard and J. R. Heath, *ChemPhysChem*, 2010, **11**, 3063–3069.
71 Y. Lu, J. J. Chen, L. Mu, Q. Xue, Y. Wu, P. H. Wu, J. Li, A. O. Vortmeyer, K. Miller-Jensen, D. Wirtz and R. Fan, *Anal. Chem.*, 2013, **85**, 2548–2556.
72 M. Kleppe, M. Kwak, P. Koppikar, M. Riester, M. Keller, L. Bastian, T. Hricik, N. Bhagwat, O. I. Abdel-Wahab, S. Marubayashi, J. J. Chen, V. Romanet, J. S. Fridman, J. Bromberg, M. Murakami, T. Radimerski, F. Michor, R. Fan and R. L. Levine, *Cancer Discovery*, 2015, **5**, 316–331.
73 J. Wang, D. Tham, W. Wei, Y. S. Shin, C. Ma, H. Ahmad, Q. Shi, J. Yu, R. D. Levine and J. R. Heath, *Nano Lett.*, 2012, **12**, 6101–6106.
74 Y. Lu, Q. Xue, M. R. Eisele, E. S. Sulistijo, K. Brower, L. Han, A. D. Amir el, D. Pe'er, K. Miller-Jensen and R. Fan, *Proc. Natl. Acad. Sci. U. S. A.*, 2015, **112**, E607–E615.
75 Q. Shi, L. Qin, W. Wei, F. Geng, R. Fan, Y. S. Shin, D. Guo, L. Hood, P. S. Mischel and J. R. Heath, *Proc. Natl. Acad. Sci. U. S. A.*, 2012, **109**, 419–424.
76 M. Xue, W. Wei, Y. P. Su, J. Kim, Y. S. Shin, W. X. Mai, D. A. Nathanson and J. R. Heath, *J. Am. Chem. Soc.*, 2015, **137**, 4066–4069.
77 B. Huang, H. Wu, D. Bhaya, A. Grossman, S. Granier, B. K. Kobilka and R. N. Zare, *Science*, 2007, **315**, 81–84.
78 A. J. Dickinson, P. M. Armistead and N. L. Allbritton, *Anal. Chem.*, 2013, **85**, 4797–4804.
79 A. J. Hughes, D. P. Spelke, Z. C. Xu, C.-C. Kang, D. V. Schaffer and A. E. Herr, *Nat. Methods*, 2014, **11**, 749–755.
80 C.-C. Kang, K. A. Yamauchi, J. Vlassakis, E. Sinkala, T. A. Duncombe and A. E. Herr, *Nat. Protoc.*, 2016, **11**, 1508–1530.
81 C.-C. Kang, M. M. Lin, Z. Xu, S. Kumar and A. E. Herr, *Anal. Chem.*, 2014, **86**, 10429–10436.
82 T. A. Duncombe, C.-C. Kang, S. Maity, T. M. Ward, M. D. Pegram, N. Murthy and A. E. Herr, *Adv. Mater.*, 2016, **28**, 327–334.
83 A. M. Tentori, K. A. Yamauchi and A. E. Herr, *Angew. Chem., Int. Ed.*, 2016, **55**, 12431–12435.
84 S. D. H. Chan, G. Luedke, M. Valer, C. Buhlmann and T. Preckel, *Cytometry, Part A*, 2003, **55**, 119–125.
85 N. Srivastava, J. S. Brennan, R. F. Renzi, M. Wu, S. S. Branda, A. K. Singh and A. E. Herr, *Anal. Chem.*, 2009, **81**, 3261–3269.
86 B. K. McKenna, J. G. Evans, M. C. Cheung and D. J. Ehrlich, *Nat. Methods*, 2011, **8**, 401–403.
87 S. Y. Teh, R. Lin, L. H. Hung and A. P. Lee, *Lab Chip*, 2008, **8**, 198–220.
88 C. Martino, M. Zagnoni, M. E. Sandison, M. Chanasakulniyom, A. R. Pitt and J. M. Cooper, *Anal. Chem.*, 2011, **83**, 5361–5368.
89 M. T. Guo, A. Rotem, J. A. Heyman and D. A. Weitz, *Lab Chip*, 2012, **12**, 2146–2155.
90 V. Chokkalingam, J. Tel, F. Wimmers, X. Liu, S. Semenov, J. Thiele, C. G. Figdor and W. T. S. Huck, *Lab Chip*, 2013, **13**, 4740–4744.
91 L. Mazutis, J. Gilbert, W. L. Ung, D. A. Weitz, A. D. Griffiths and J. A. Heyman, *Nat. Protoc.*, 2013, **8**, 870–891.
92 B. El Debs, R. Utharala, I. V. Balyasnikova, A. D. Griffiths and C. A. Merten, *Proc. Natl. Acad. Sci. U. S. A.*, 2012, **109**, 11570–11575.
93 S. Akbari and T. Pirbodaghi, *Lab Chip*, 2014, **14**, 3275–3280.
94 D. M. Rissin, C. W. Kan, T. G. Campbell, S. C. Howes, D. R. Fournier, L. N. Song, T. Piech, P. P. Patel, L. Chang, A. J. Rivnak, E. P. Ferrell, J. D. Randall, G. K. Provuncher, D. R. Walt and D. C. Duffy, *Nat. Biotechnol.*, 2010, **28**, 595–599.
95 S. M. Schubert, S. R. Walter, M. Manesse and D. R. Walt, *Anal. Chem.*, 2016, **88**, 2952–2957.
96 B. Mascher, P. Schlenke and M. Seyfarth, *J. Immunol. Methods*, 1999, **223**, 115–121.
97 E. W. Newell, N. Sigal, S. C. Bendall, G. P. Nolan and M. M. Davis, *Immunity*, 2012, **36**, 142–152.
98 M. Junkin, A. J. Kaestli, Z. Cheng, C. Jordi, C. Albayrak, A. Hoffmann and S. Tay, *Cell Rep.*, 2016, **15**, 411–422.
99 Q. Xue, Y. Lu, M. R. Eisele, E. S. Sulistijo, N. Khan, R. Fan and K. Miller-Jensen, *Sci. Signaling*, 2015, **8**, ra59.

100 N. Kravchenko-Balashaa, Y. S. Shin, A. Sutherland, R. D. Levine and J. R. Heath, *Proc. Natl. Acad. Sci. U. S. A.*, 2016, **113**, 5520–5525.
101 C. Ma, A. F. Cheung, T. Chodon, R. C. Koya, Z. Wu, C. Ng, E. Avramis, A. J. Cochran, O. N. Witte, D. Baltimore, B. Chmielowski, J. S. Economou, B. Comin-Anduix, A. Ribas and J. R. Heath, *Cancer Discovery*, 2013, **3**, 418–429.
102 F. C. Lam and M. B. Yaffe, *Cancer Cell*, 2016, **29**, 435–436.
103 C. W. Brennan, R. G. W. Verhaak, A. McKenna, B. Campos, H. Noushmehr, S. R. Salama, S. Zheng, D. Chakravarty, J. Z. Sanbom, S. H. Berman, R. Beroukhim, B. Bernard, C. Wu, G. Genovese, I. Shmulevich, J. Barnholtz-Sloan, L. Zou, R. Vegesna, S. A. Shukla, G. Ciriello, W. K. Yung, W. Zhang, C. Sougnez, T. Mikkelsen, K. Aldape, D. D. Bigner, E. G. Van Meir, M. Prados, A. Sloan, K. L. Black, J. Eschbacher, G. Finocchiaro, W. Friedman, D. W. Andrews, A. Guha, M. Iacocca, B. P. O'Neill, G. Foltz, J. Myers, D. J. Weisenberger, R. Penny, R. Kucherlapati, C. M. Perou, D. N. Hayes, R. Gibbs, M. Marra, G. B. Mills, E. Lander, P. Spellman, R. Wilson, C. Sander, J. Weinstein, M. Meyerson, S. Gabrie, P. W. Laird, D. Haussler, G. Getz and L. Chin, *Cell*, 2013, **155**, 462–477.
104 C. G. Begley and L. M. Ellis, *Nature*, 2012, **483**, 531–533.
105 M. Baker, *Nature*, 2015, **521**, 274–276.

